E-Component – Energy and Reserve Dispatch with Distributionally Robust Joint Chance Constraints

CHRISTOS ORDOUDIS, VIET ANH NGUYEN, DANIEL KUHN, PIERRE PINSON

This electronic component (EC) to the paper "Energy and Reserve Dispatch with Distributionally Robust Joint Chance Constraints" [1] describes the nomenclature, the collective optimization model of [1, Section 5], the IEEE 24-bus Reliability Test System, the procedure to generate wind power data, the parameters underlying the numerical simulations and some auxiliary results on the Bonferroni and CVaR approximations.

A. Nomenclature

Table T.1 lists all symbols that appear in [1] and provides for each of them a short description.

Table T.1. Nomenclature

Symbol	Description
y_1	First-stage power dispatch of conventional power plants
Y	Coefficient matrix of the affine policy of the conventional power plants' real time adjustments
r_-	Downward reserve capacity of conventional power plants
r_+	Upward reserve capacity of conventional power plants
μ	Predicted power production of the wind farms
ξ	Random variable with zero mean
C	Diagonal matrix of wind farm capacities
Q	Matrix of power transfer distribution factors
$\overline{r}$	Maximum reserve capacity offered by conventional power plants
$\overline{y}$	Maximum power production of conventional power plants
$\underline{y}$	Minimum power production of conventional power plants
$\overline{\overline{f}}$	Capacity limits of transmission lines
$\overline{q}$	Capacity limits of pipelines
Φ	Matrix of gas transfer distribution factors
d	Electricity demands
c	Variable costs of conventional power plants
c_-	Cost of reserving downward capacity
c_+	Cost of reserving upward capacity
e	Vector of ones
ϵ	Violation probabilities of joint chance constraints
$\mathbb{P}$	True probability distribution of the random vector ξ
$\widehat{\mathbb{P}}_N$	Empirical distribution on the training samples
N	Number of training samples
M	Number of test samples
$\mathcal{P}$	Wasserstein ambiguity set
ρ	Wasserstein radius
δ	Vector of scaling parameters for the optimized CVaR approximation
η	Minimum relative improvement per iteration in the sequential optimization algorithm
v	Auxiliary slack variables for the joint chance constraints
M	Big-M constant

B. Collective Optimization Model

Denote by $\mathcal{P} \triangleq \{\mathbb{P} \in \mathcal{M}(\Xi) : \mathbb{W}(\mathbb{P}, \widehat{\mathbb{P}}_N) \leq \rho\}$ the Wasserstein ambiguity set of radius ρ. In this section we provide a formal description of the collective optimization model and explain how it can be approximated by a tractable convex program both for $\rho > 0$ and for $\rho = 0$.

The collective optimization model constitutes a two-stage distributionally robust optimization problem reminiscent of [1, Equation (1)] that minimizes the worst-case expected cost with respect to all probability distributions in $\mathcal{P}$, while enforcing the constraints robustly for all uncertainty realizations within the box uncertainty set $\Xi = \{\xi \in \mathbb{R}^W : -\mu \leq \xi \leq e - \mu\}$. More precisely, the collective optimization model is formulated as

$$\begin{array}{lll}
\min\limits_{\substack{y_1, r_+, r_- \\ y_2(\cdot), r(\cdot), l(\cdot), w(\cdot)}} & c^\top y_1 + c_+^\top r_+ + c_-^\top r_- + \max\limits_{\mathbb{P}\in\mathcal{P}} \mathbb{E}^{\mathbb{P}}[c^\top y_2(\xi) + c_r e^\top r(\xi) + c_w e^\top w(\xi) + c_l e^\top l(\xi)] & \\
\text{s.t.} & 0 \leq r_+ \leq \overline{r}, \quad 0 \leq r_- \leq \overline{r} & \\
& \underline{y} \leq y_1 - r_-, \quad y_1 + r_+ \leq \overline{y} & \\
& e^\top C(\mu + \xi) - e^\top w(\xi) + e^\top (y_1 + y_2(\xi)) = e^\top (d - l(\xi)) & \forall \xi \in \Xi \\
& -(r_- + r(\xi)) \leq y_2(\xi) \leq r_+ & \forall \xi \in \Xi \\
& -\overline{f} \leq Q^{\mathrm{g}}(y_1 + y_2(\xi)) + Q^{\mathrm{w}} C(\mu + \xi - w(\xi)) - Q^{\mathrm{d}}(d - l(\xi)) \leq \overline{f} & \forall \xi \in \Xi \\
& 0 \leq \Phi(y_1 + y_2(\xi)) \leq \overline{q} & \forall \xi \in \Xi \\
& 0 \leq r(\xi), \quad 0 \leq w(\xi) \leq C(\mu + \xi), \quad 0 \leq l(\xi) \leq d & \forall \xi \in \Xi.
\end{array}$$

Notably, the collective optimization problem also includes additional flexibility in choosing reserve increment $r(\xi)$, wind spilling $w(\xi)$, and load shedding $l(\xi)$ at appropriate nodes in the system. These additional decisions are penalized with some positive parameters c_r, c_w and c_l, respectively. The objective function and the constraints of this problem can be explained in a similar manner as in [1, Section 2].

B.1. Strictly Positive Wasserstein Radius

If $\rho > 0$, we restrict the adaptive functional decisions to linear decision rules of the form $y_2(\xi) = Y\xi$, $r(\xi) = Y_2\xi$, $w(\xi) = Y_3\xi$ and $l(\xi) = Y_4\xi$ for some matrices $Y \in \mathbb{R}^{G\times W}$, $Y_2 \in \mathbb{R}^{G\times W}$, $Y_3 \in \mathbb{R}^{W\times W}$ and $Y_4 \in \mathbb{R}^{D\times W}$, respectively, to obtain the following linear decision rule approximation

$$\begin{array}{lll}
\min\limits_{\substack{y_1, r_+, r_- \\ Y, Y_2, Y_3, Y_4}} & c^\top y_1 + c_+^\top r_+ + c_-^\top r_- + \max\limits_{\mathbb{P}\in\mathcal{P}} \mathbb{E}^{\mathbb{P}}[(c^\top Y + c_l e^\top Y_4 + c_w e^\top Y_3 + c_r e^\top Y_2)\xi] & \\
\text{s.t.} & 0 \leq r_+ \leq \overline{r}, \quad 0 \leq r_- \leq \overline{r} & \\
& \underline{y} \leq y_1 - r_-, \quad y_1 + r_+ \leq \overline{y} & \\
& e^\top C(\mu + \xi) - e^\top Y_3\xi + e^\top (y_1 + Y\xi) = e^\top (d - Y_4\xi) & \forall \xi \in \Xi \\
& -(r_- + Y_2\xi) \leq Y\xi \leq r_+ & \forall \xi \in \Xi \\
& -\overline{f} \leq Q^{\mathrm{g}}(y_1 + Y\xi) + Q^{\mathrm{w}} C(\mu + \xi - Y_3\xi) - Q^{\mathrm{d}}(d - Y_4\xi) \leq \overline{f} & \forall \xi \in \Xi \\
& 0 \leq \Phi(y_1 + Y\xi) \leq \overline{q} & \forall \xi \in \Xi \\
& 0 \leq Y_2\xi, \quad 0 \leq Y_3\xi \leq C(\mu + \xi), \quad 0 \leq Y_4\xi \leq d & \forall \xi \in \Xi.
\end{array}$$

The above semi-infinite program can be reformulated more concisely as

$$\begin{array}{lll}
\min\limits_{\substack{y_1, r_+, r_- \\ Y, Y_2, Y_3, Y_4}} & c^\top y_1 + c_+^\top r_+ + c_-^\top r_- + \max\limits_{\mathbb{P}\in\mathcal{P}} \mathbb{E}^{\mathbb{P}}[(c^\top Y + c_l e^\top Y_4 + c_w e^\top Y_3 + c_r e^\top Y_2)\xi] & \\
\text{s.t.} & 0 \leq r_+ \leq \overline{r}, \quad 0 \leq r_- \leq \overline{r}, \quad \underline{y} \leq y_1 - r_-, \quad y_1 + r_+ \leq \overline{y} & \\
& e^\top y_1 + e^\top C\mu = e^\top d, \quad e^\top Y + e^\top C - e^\top Y_3 + e^\top Y_4 = 0 & \\
& [A^j(Y) + A_2^j(Y_2) + A_3^j(Y_3) + A_4^j(Y_4)]\xi \leq b^j(x) & \forall \xi \in \Xi, \forall j \in \mathcal{J} \\
& 0 \leq Y_2\xi, \quad 0 \leq Y_3\xi \leq C(\mu + \xi), \quad 0 \leq Y_4\xi \leq d & \forall \xi \in \Xi,
\end{array}$$

where $\mathcal{J} \triangleq \{\text{gen}, \text{grid}, \text{gas}\}$, and $x \triangleq (y_1, r_+, r_-) \in \mathbb{R}^{3G}_+$ denotes the collection of all first-stage decisions. Furthemore, the functions $A^j(Y)$ and $b^j(x)$ are defined as in [1], that is, for the generator constraints we have

$$A^{\text{gen}}(Y) \triangleq \begin{bmatrix} Y \\ -Y \end{bmatrix}, \quad b^{\text{gen}}(x) \triangleq \begin{bmatrix} r_+ \\ -r_- \end{bmatrix},$$

for the grid line capacity constraints we have

$$A^{\text{grid}}(Y) \triangleq \begin{bmatrix} Q^{\text{g}}Y + Q^{\text{w}}C \\ -Q^{\text{g}}Y - Q^{\text{w}}C \end{bmatrix}, \quad b^{\text{grid}}(x) \triangleq \begin{bmatrix} \overline{f} - Q^{\text{w}}C\mu + Q^{\text{d}}d - Q^{\text{g}}y_1 \\ \overline{f} + Q^{\text{w}}C\mu - Q^{\text{d}}d + Q^{\text{g}}y_1 \end{bmatrix},$$

and for the pipeline capacity constraints we have

$$A^{\text{gas}}(Y) \triangleq \begin{bmatrix} \Phi Y \\ -\Phi Y \end{bmatrix}, \quad b^{\text{gas}}(x) \triangleq \begin{bmatrix} \overline{q} - \Phi y_1 \\ \Phi y_1 \end{bmatrix}.$$

For the reserve increment variables Y_2, we have the corresponding mappings

$$A_2^{\text{gen}}(Y_2) = \begin{bmatrix} \mathbf{0} \\ -Y_2 \end{bmatrix}, \quad A_2^{\text{grid}}(Y_2) = \begin{bmatrix} \mathbf{0} \\ \mathbf{0} \end{bmatrix}, \quad A_2^{\text{gas}}(Y_2) = \begin{bmatrix} \mathbf{0} \\ \mathbf{0} \end{bmatrix}.$$

In a similar manner, the mappings for the wind spillage variables Y_3 and load shedding variables Y_4 are

$$A_3^{\text{gen}}(Y_3) = \begin{bmatrix} \mathbf{0} \\ \mathbf{0} \end{bmatrix}, \quad A_3^{\text{grid}}(Y_3) = \begin{bmatrix} -Q^{\text{w}}Y_3 \\ Q^{\text{w}}Y_3 \end{bmatrix}, \quad A_3^{\text{gas}}(Y_3) = \begin{bmatrix} \mathbf{0} \\ \mathbf{0} \end{bmatrix},$$
$$A_4^{\text{gen}}(Y_4) = \begin{bmatrix} \mathbf{0} \\ \mathbf{0} \end{bmatrix}, \quad A_4^{\text{grid}}(Y_4) = \begin{bmatrix} Q^{\text{d}}Y_4 \\ -Q^{\text{d}}Y_4 \end{bmatrix}, \quad A_4^{\text{gas}}(Y_4) = \begin{bmatrix} \mathbf{0} \\ \mathbf{0} \end{bmatrix}.$$

As the box uncertainty set Ξ has 2^W vertices, we can replace each robust constraint with 2^W classical linear constraints corresponding to the vertices ξ_{v} of Ξ, $\text{v} = 1, \ldots, 2^W$. The semi-infinite optimization problem obtained from the decision rule approximation can thus be re-expressed as the following linear distributionally robust optimization problem.

$$\begin{array}{lll}
\min\limits_{\substack{y_1, r_+, r_- \\ Y, Y_2, Y_3, Y_4}} & c^\top y_1 + c_+^\top r_+ + c_-^\top r_- + \max\limits_{\mathbb{P} \in \mathcal{P}} \mathbb{E}^{\mathbb{P}}[(c^\top Y + c_r e^\top Y_2 + c_w e^\top Y_3 + c_l e^\top Y_4)\xi] & \\
\text{s. t.} & 0 \le r_+ \le \overline{r}, \quad 0 \le r_- \le \overline{r}, \quad \underline{y} \le y_1 - r_-, \quad y_1 + r_+ \le \overline{y} & \\
& e^\top y_1 + e^\top C\mu = e^\top d, \quad e^\top Y + e^\top C - e^\top Y_3 + e^\top Y_4 = 0 & \\
& [A^j(Y) + A_2^j(Y_2) + A_3^j(Y_3) + A_4^j(Y_4)]\xi_{\text{v}} \le b^j(x) & \forall \text{v} = 1, \ldots, 2^W, \forall j \in \mathcal{J} \\
& 0 \le Y_2\xi_{\text{v}}, \quad 0 \le Y_3\xi_{\text{v}} \le C(\mu + \xi_{\text{v}}), \quad 0 \le Y_4\xi_{\text{v}} \le d & \forall \text{v} = 1, \ldots, 2^W.
\end{array}$$

We now consider the reformulation of the worst-case expected loss of the collective optimization problem. Similar to the results of [1, Section 4.1], we find

$$\begin{aligned}
&\max_{\mathbb{P} \in \mathcal{P}} \mathbb{E}^{\mathbb{P}}[(c^\top Y + c_r e^\top Y_2 + c_w e^\top Y_3 + c_l e^\top Y_4)\xi] \\
&= \left\{ \begin{array}{lll}
\min\limits_{\lambda^o, s^o, \gamma^o} & \lambda^o \rho + N^{-1} \sum_{i=1}^N s_i^o & \\
\text{s. t.} & (c^\top Y + c_r e^\top Y_2 + c_w e^\top Y_3 + c_l e^\top Y_4)\widehat{\xi}_i + \gamma_i^{o\top}(h - H\widehat{\xi}_i) \le s_i^o & \forall i \le N \\
& \|H^\top \gamma_i^o - Y^\top c - c_r Y_2^\top e - c_w Y_3^\top e - c_l Y_4^\top e\|_* \le \lambda^o & \forall i \le N \\
& \gamma_i^o \in \mathbb{R}^{2W}_+ & \forall i \le N \\
& \lambda^o \in \mathbb{R}_+, \ s^o \in \mathbb{R}^N, &
\end{array} \right.
\end{aligned}$$

where $\|\cdot\|_*$ stands for the dual norm of $\|\cdot\|$. The collective optimization problem thus can be reformulated as a tractable conic program.

B.2. **Zero Wasserstein Radius**

If $\rho = 0$, then the collective optimization model collapses to the sample average approximation problem

$$
\begin{array}{lll}
\min\limits_{\substack{y_1,r_+,r_-\\ y_2,r,l,w}} & c^\top y_1 + c_+^\top r_+ + c_-^\top r_- + N^{-1}\sum_{i=1}^N \left(c^\top y_{2i} + c_r e^\top r_i + c_l e^\top l_i + c_w e^\top w_i\right) & \\
\text{s.t.} & 0 \le r_+ \le \overline{r}, \quad 0 \le r_- \le \overline{r}, \quad \underline{y} \le y_1 - r_-, \quad y_1 + r_+ \le \overline{y} & \\
& 0 \le y_1 + y_{2i} \le \overline{y},\ -(\widehat{r}_- + r_i) \le y_{2i} \le \widehat{r}_+ & \forall i = 1,\ldots,N \\
& e^\top y_1 + e^\top C\mu = e^\top d & \\
& e^\top y_{2i} + e^\top (C\widehat{\xi}_i - w_i) + e^\top l_i = 0 & \forall i = 1,\ldots,N \\
& r_- \le y_{2i} \le r_+ & \forall i = 1,\ldots,N \\
& -\overline{f} \le Q^{\mathrm{g}}(y_1 + y_{2i}) + Q^{\mathrm{w}}(C\mu + C\widehat{\xi}_i - w_i) - Q^{\mathrm{d}}(d - l_i) \le \overline{f} & \forall i = 1,\ldots,N \\
& 0 \le \Phi(y_1 + y_{2i}) \le \overline{q} & \forall i = 1,\ldots,N \\
& 0 \le r_i \le y_1 - r_-, 0 \le l_i \le d,\ 0 \le w_i \le C(\mu + \widehat{\xi}_i) & \forall i = 1,\ldots,N.
\end{array}
$$

We emphasize that this model accommodates separate second-stage decisions (y_{2i}, r_i, l_i, w_i) for each sample $\widehat{\xi}_i$, $i = 1,\ldots,N$ and constitutes a linear program that can be solved with off-the-shelf software packages. The out-of-sample performance of the collective optimization model is evaluated on the test samples $\widehat{\xi}_i$, $i = N+1,\ldots,N+M$ using the procedure described in [1, Section 5].

C. Data for the IEEE 24-bus RTS

We now provide the details regarding the data used in the numerical experiment of [1, Section 5]. The 24-bus power system, of which the slack bus is bus 13, is illustrated in Figure F.1. Tables T.2-T.4, adopted from [2, 3], summarize the configurations of the power generating units, the demand and the electricity grid. Table T.2 provides the technical data of generating units, including the location on the power system, the relevant costs, as well as the conversion factor and the connection with the corresponding pipelines for the gas-fired power plants. The generating units of the power system offer a single block of energy, along with up and down reserve capacity. There are three pipelines that the gas-fired power plants (GFPPs) are connected to, and the capacity of the gas pipelines is adopted from capacity of pipelines are based on the test case used in [2]: Pipeline 1 has a capacity of 10,000 kcf, Pipeline 2 has a capacity of 5,500 kcf and Pipeline 3 has a capacity of 7,000 kcf (kcf: 1,000 cubic feet). The marginal cost of power production c in Table T.2 are modified so that each power plant has a different cost to prioritize the order of dispatch.

Concerning the electricity demand, Table T.3 presents the bus location of the loads, as well as the load at each bus as a percentage of the total system demand. The total electricity demand over the whole grid is 2,650 MWh. Table T.4 contains the necessary information regarding the electricity transmission lines. Each line is characterized by the buses that it connects, as well as the reactance and the transmission capacity. There are 6 wind farms of nominal capacity 250 MW connected to the electricity grid at bus 1, 2, 11, 12, 12, 16, respectively.

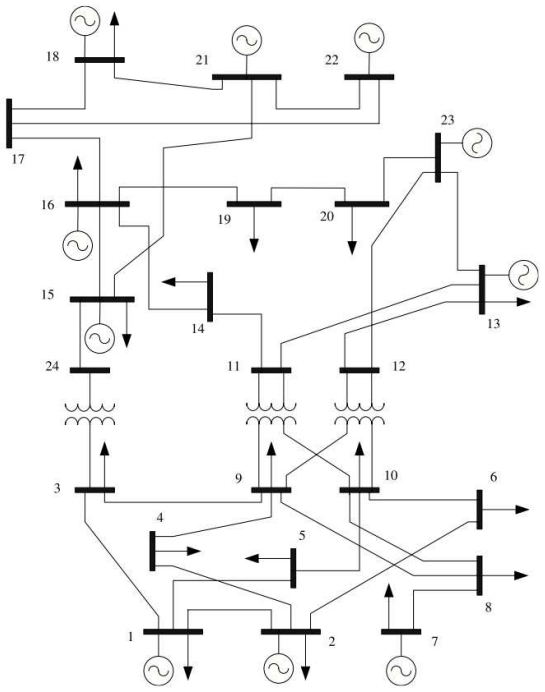

FIGURE F.1. 24-bus power system – Single area RTS-96

TABLE T.2. Technical data of electricity generating units

Unit #	Bus	$\overline{y}$ (MW)	$\underline{y}$ (MW)	$\overline{r}$ (MW)	c (\$/MWh)	c_+ (\$/MW)	c_- (\$/MW)	Φ (kcf/MWh)	Pipeline
1	1	152	0	60.8	17.5	3.5	3.5	12.65	1
2	2	152	0	60.8	20	4	4	13.45	3
3	7	300	0	120	15	3	3	-	-
4	13	591	0	236.4	27.5	5.5	5.5	-	-
5	15	60	0	24	30	6	6	11.12	2
6	15	155	0	62	22.5	4.5	4.5	-	-
7	16	155	0	62	25	5	5	14.88	1
8	18	400	0	160	5	1	1	-	-
9	21	400	0	160	7.5	1.5	1.5	-	-
10	22	300	0	120	32.5	6.5	6.5	-	-
11	23	310	0	124	10	2	2	16.8	2
12	23	350	0	140	12.5	2.5	2.5	15.6	3

TABLE T.3. Bus location and distribution of the total system demand

Load #	Bus	% of system load	Load #	Bus	% of system load
1	1	3.8	10	10	6.8
2	2	3.4	11	13	9.3
3	3	6.3	12	14	6.8
4	4	2.6	13	15	11.1
5	5	2.5	14	16	3.5
6	6	4.8	15	18	11.7
7	7	4.4	16	19	6.4
8	8	6	17	20	4.5
9	9	6.1			

TABLE T.4. Reactance and capacity of the transmission lines

From	To	Reactance (p.u.)	Capacity (MW)	From	To	Reactance (p.u.)	Capacity (MW)
1	2	0.0146	175	11	13	0.0488	500
1	3	0.2253	175	11	14	0.0426	500
1	5	0.0907	400	12	13	0.0488	500
2	4	0.1356	175	12	23	0.0985	500
2	6	0.205	175	13	23	0.0884	500
3	9	0.1271	400	14	16	0.0594	1000
3	24	0.084	200	15	16	0.0172	500
4	9	0.111	175	15	21	0.0249	1000
5	10	0.094	400	15	24	0.0529	500
6	10	0.0642	400	16	17	0.0263	500
7	8	0.0652	600	16	19	0.0234	500
8	9	0.1762	175	17	18	0.0143	500
8	10	0.1762	175	17	22	0.1069	500
9	11	0.084	200	18	21	0.0132	1000
9	12	0.084	200	19	20	0.0203	1000
10	11	0.084	200	20	23	0.0112	1000
10	12	0.084	200	21	22	0.0692	500

D. WIND POWER DATA GENERATION FOR THE SIMULATION OF NUMERICAL RESULTS

The data consists of wind power forecast errors that is generated with the same method and the historical data given in [4]. The wind power data are provided by the Australian System Operator [5], which consists of wind power generation recordings from 22 wind farms in the southeastern Australia. The complete dataset can be found in [6]. Data from 2012 and 2013 are normalized by the nominal power of the corresponding wind farm which results in data being in the range of $[0, 1]$. From the csv file that is publicly available in [6], we have chosen the 6 wind farms presented in Table T.5.

The wind power data are generated with the following procedure.

(1) Load the 2 years of raw data for the 6 chosen wind farms.
(2) Project each data point to the range $[0.01, 0.99]$, then apply a logit-normal transformation (see [4, Equation (1)]).
(3) Calculate the sample mean $\widehat{\mu}$ and the sample covariance matrix $\widehat{\Sigma}$ from the transformed data.

TABLE T.5. Wind farm locations and name tags in the csv file

WF	Bus	Name tag in csv
1	1	CAPTL_WF
2	2	CATHROCK
3	11	CULLRGWF
4	12	LKBONNY1
5	12	MTMILLAR
6	16	STARHLWF

(4) Generate the required number of independent and identically distributed random samples by assuming that the transformed variables are normally distributed with distribution $\mathcal{N}(\widehat{\mu}, \widehat{\Sigma})$.
(5) Apply the inverse logit-normal transformation (see [4, Equation (2)]) on the samples obtained from the previous step.

We refer the readers to [4] for a detailed presentation of the method and additional insights on the very-short-term probabilistic wind power forecasting. Note that the procedure can be found also in the source code provided online at https://github.com/nvietanh/DR_JCC.

E. DATA FOR THE SIMULATION OF NUMERICAL RESULTS

The discretized search space of ρ for the Bonferroni and CVaR approximation is confined to the vector $\{0,\ \text{linspace}(10^{-4}, 24 \cdot 10^{-4}, 23)\}$, while the discretized search space for the optimized CVaR approximation is $\{0,\ 10^{-4},\ \text{linspace}(10^{-3}, 10^{-2}, 23)\}$. The MATLAB command $\text{linspace}(a, b, n)$ generates n points evenly distributed on the interval $[a, b]$. Table T.6 presents the values of the parameters related to the algorithm utilized in the optimized CVaR approximation of distributionally robust joint chance constraints.

TABLE T.6. Parameters for the sequential algorithm to solve the optimized CVaR approximation problem described in [1, Section 4.3]

Parameter	Description	Numerical value
$\bar{t}$	Number of iterations	40
η	Objective value improvement tolerance	0.1
M	Big-M constant	10^6

F. ADDITIONAL RESULTS FOR THE BONFERRONI AND CVAR APPROXIMATION APPROACH

Figures F.2 and F.3 illustrate the impact of Wasserstein radius ρ on the expected value and interquantile range between the 10^{th}- and 90^{th}-quantiles of the empirical cost $\widehat{C}$ using reoptimization. These two figures are the corresponding counterparts of Figures 2 and 3 in the original manuscript [1] for the Bonferroni and CVaR approximation approach.

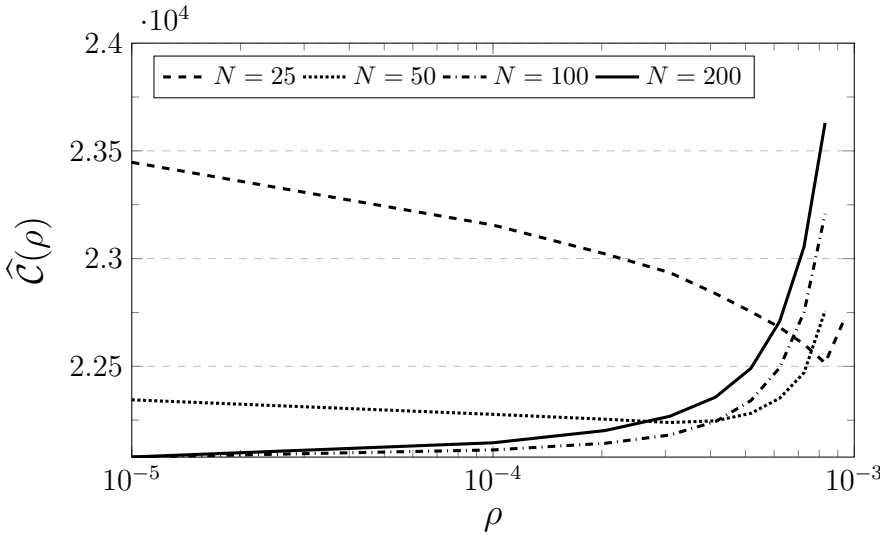

FIGURE F.2. Average out-of-sample cost $\widehat{\mathcal{C}}(\rho)$ using the Bonferroni and CVaR approximation and reoptimization.

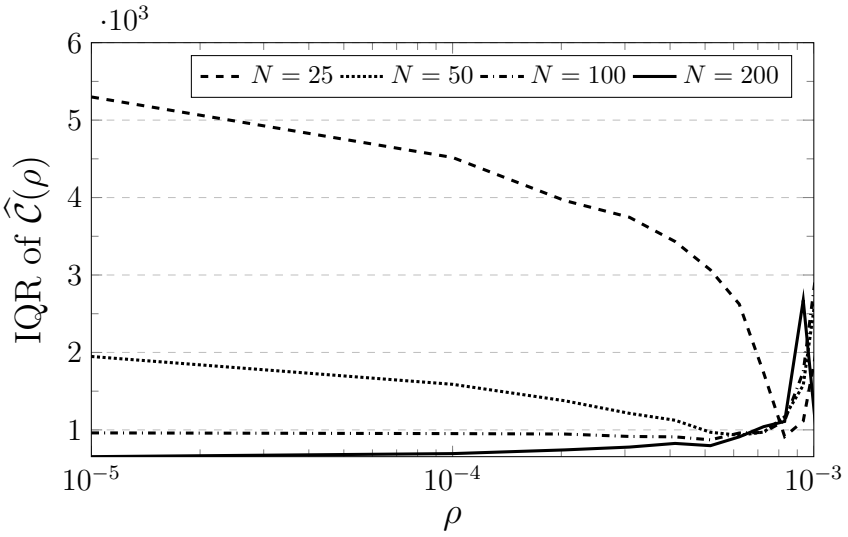

FIGURE F.3. Interquantile range between the empirical 10^{th}- and 90^{th}-quantiles of $\widehat{\mathcal{C}}(\rho)$ using the Bonferroni and CVaR approximation and reoptimization.

REFERENCES

[1] C. Ordoudis, V. A. Nguyen, D. Kuhn, and P. Pinson, "Energy and reserve dispatch with distributionally robust joint chance constraints," *Working paper*, 2019.

[2] C. Ordoudis, P. Pinson, and J. M. Morales, "An integrated market for electricity and natural gas systems with stochastic power producers," *Eur. J. Oper. Res.*, vol. 272, no. 2, pp. 642 – 654, 2019.

[3] J. M. Morales, A. J. Conejo, H. Madsen, P. Pinson, and M. Zugno, *Integrating Renewables in Electricity Markets: Operational Problems*. International Series in Operations Research & Management Science, Springer US, 2014.

[4] J. Dowell and P. Pinson, "Very-short-term probabilistic wind power forecasts by sparse vector autoregression," *IEEE Trans. Smart Grid*, vol. 7, no. 2, pp. 763–770, 2016.

[5] Australian Energy Market Operator, "AEMO wind power data." http://www.aemo.com.au/, 2019. Online; Accessed: 25.12.2019.

[6] J. Browell, "AEMO wind power data." http://www.jethrobrowell.com/data-and-code.html, 2019. Online; Accessed: 25.12.2019.